Inorganic Chemistry

ARTICLE

pubs.acs.org/IC

Phase Transformation and Negative Thermal Expansion in $TaVO_5$

Xiaowei Wang,[†] Qingzhen Huang,[‡] Jinxia Deng,[†,§] Ranbo Yu,[†] Jun Chen,[†] and Xianran Xing*[,†]

[†]Department of Physical Chemistry, University of Science and Technology Beijing, Beijing 100083, China

[‡]NIST Center for Neutron Research, National Institute of Standards and Technology, Gaithersburg, Maryland 20899-6102, United States

[§]Department of Chemistry, University of Science and Technology Beijing, Beijing 100083, China

S Supporting Information

ABSTRACT: Two phase transformations of $TaVO_5$ were observed by DSC and/or dilatometry measurements in the studied temperature range. X-ray diffraction and neutron powder diffraction structure refinements indicated a phase transformation at −14 °C from a monoclinic symmetry with space group $P2_1/c$ to an orthorhombic symmetry with space group *Pnma* above this temperature. The rigid TaO_6 octahedron in orthorhombic phase becomes nonregular at −14 °C, which results in the transition from *Pnma* to $P2_1/c$. $TaVO_5$ was found to be a negative thermal expansion material above room temperature. The calculated volumetric thermal expansion coefficients (TECs) are -8.92×10^{-6} °C^{-1} in the range of 20−600 °C, and -2.19×10^{-5} °C^{-1} above 600 °C, respectively. The negative thermal expansion behavior is accounted for by the tilt of the TaO_6 and VO_4 polyhedra, where the shrinkage of the VO_4 tetrahedra result in the increase of Ta−O−V angles on heating, while the angle of Ta−O1−Ta maintains at 180° in the framework.

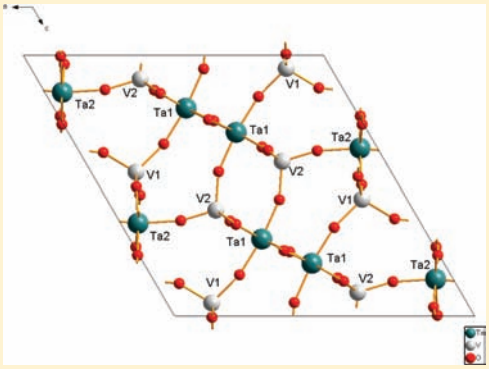

INTRODUCTION

The compounds with monophosphate tungsten bronze structure (MPTB) $(PO_2)_4(WO_3)_{2m}$ (m = 2) are a big family, and one of the simple forms ABO_5 (simplified from $(BO_2)_4(AO_3)_4$) is composed of BO_6 octahedra and AO_4 tetrahedra connected by sharing the corner oxygen, where A and B are cations in the polyhedra.[1−3] The big pentagonal tunnels formed with two tetrahedral and three octahedral in a framework structure permit small atoms or particles to enter into the space, which could be used as an intercalation material such as Li-battery anode or a catalyst material.[4−6] Such structure flexibility also makes its thermal expansion become negative possibly. For example, the negative thermal expansion (NTE) of orthorhombic $NbPO_5$ was observed above 400 °C.[7]

The structure of $TaVO_5$ was refined with XRD data to be isomorphous to orthorhombic $NbPO_5$ with space group *Pnma*.[8] Several groups measured the thermal expansion coefficients (TEC) of $TaVO_5$ by dilatometers, -4.0×10^{-6} °C^{-1} above room temperature (RT),[9] and -4.0×10^{-6} °C^{-1} above 260 K, and 50.0×10^{-6} °C^{-1} below.[10] The consecutive systematic studies showed -4.1×10^{-6} °C^{-1} for linear TEC by dilatometry and -1.5×10^{-5} °C^{-1} for volumetric TEC by XRD measurements in the temperature ranges of RT to 800 °C and RT to 600 °C, respectively.[11] The NTE behavior was attributed to the tilting and rotations of the corner-shared TaO_6 and VO_4 polyhedra. However, both dilatometry and DSC measurements suggest a phase transformation around 260 K,[9−11] and its transformation mechanism and structure below this temperature have not yet been elucidated. Moreover, the refined structure informative data determined by XRD and neutron powder diffraction methods with elevated temperatures are necessary to further reveal the facts for NTE and phase transformation.

In the present work, DSC was used to detect a phase transition and thermal evolution. The XRD and neutron powder diffraction (NPD) were incorporated to determine the structure at various temperatures. The TECs were determined both by XRD and dilatometry methods.

EXPERIMENTAL SECTION

$TaVO_5$ was prepared by a solid-state reaction method using analytic reagent grade raw materials V_2O_5 and Ta_2O_5. Starting reagents with the molar ratio of V_2O_5/Ta_2O_5 = 0.52:0.48 were ball-milled in ethanol for 10 h. The dried and mixed powders were pressed into pellets of 11-mm diameter and 2−3-mm thickness and then calcined at 800 °C for 24 h. The excess V_2O_5 is to compensate for its evaporation loss during heating. The pellets cooled in the furnace were ground into powders, and then annealed at 550 °C for 1 h to remove the mechanical strain introduced during the sintering and grinding processes.

An advanced analyzer (NETZSCH DIL 402C) was used for accurate dilatometric cycle running measurements with a rate of 5 °C·min^{-1} from RT to 600 °C. A ceramic bar (28 mm × 5 mm × 3 mm) was pressed and sintered at 800 °C for 24 h before the dilatometric

Received: January 2, 2011
Published: February 21, 2011

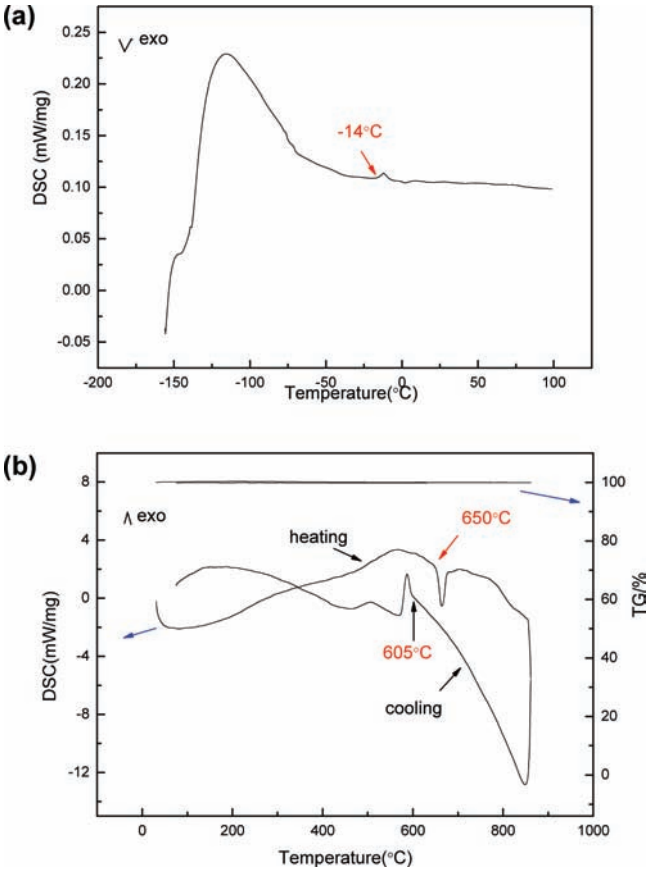

Figure 1. (a) DSC measurements of $TaVO_5$ in the temperature range −150 to 100 °C. (b) DSC measurements of $TaVO_5$ in the temperature range RT to 850 °C.

determination. DSC measurements were carried out on a Setaram Labsys Evo from RT to 800 °C and a Netzsch Sta409 with liquid nitrogen cooling below RT.

Phase identification and structural characterization were conducted from X-ray diffraction (XRD) technique on a 21 kW extra-power powder diffractometer with Cu Kα radiation using Si as internal standard (model M21XVHF22, Mac Science, Yokohama, Japan). For high-temperature measurements, the scanning speed of 2θ angle was 5 °C·min^{-1} and the heating speed was 15 °C·min^{-1}. The XRD data below RT were recorded on a diffractometer (Rigaku D/MAX, Japan). Neutron powder diffraction data were collected on the BT-1 diffractometer at the center for Neutron Research at the National Institute of Standards and Technology with a Cu monochromator (λ = 1.5403 Å) at −100, 20, and 400 °C. The lattice parameters were calculated by a combination of Rietveld and Lebail methods in Fullprof and all structure refinements were performed using Fullprof software.

RESULTS AND DISCUSSION

According to the phase diagram of the V_2O_5−Ta_2O_5 system, $TaVO_5$ is an incongruent melting compound and will be decomposed above 1027 °C.[12] Actually we prepared the pure orthorhombic $TaVO_5$ by mixing starting oxides V_2O_5 and Ta_2O_5 and sintering at 800 °C. Higher sintering temperature will lead to introducing an impurity. DSC measurement below RT showed an endothermal peak at −14 °C (see Figure 1a), which was suggested as a phase transformation by previous researchers.[9−11] Our further DSC data above RT, however, demonstrated another phase transformation around 600 °C, which has never been reported (see Figure 1b). The dilatometric measurements also confirmed the existence of this phase transformation, where the slope of thermal expansion abruptly decreased on heating and jumped on cooling around 600 °C (see Figure S1 in the Supporting Information). Therefore, dilatometric data were collected over a temperature range of RT to 600 °C in one thermal circle measurements, and an average linear thermal expansion coefficient is -3.69×10^{-6} °C^{-1} (see Figure 2).

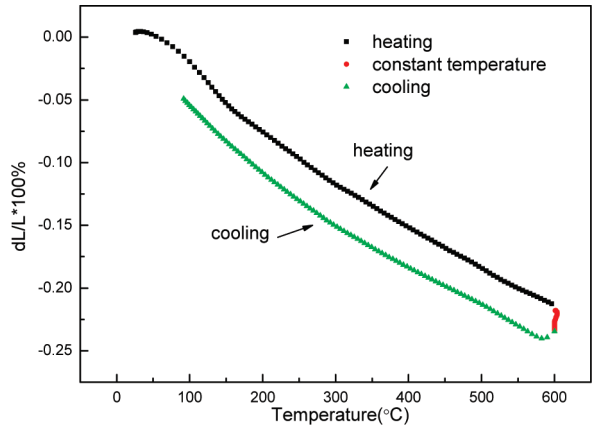

Figure 2. Dilatometric measurements of $TaVO_5$ from RT to 600 °C.

Table 1. Thermal Expansion Coefficients of $TaVO_5$

temperature range (°C)	cell dimension	α (° C^{-1})
−150−20	*a*	-7.34×10^{-6}
	b	3.00×10^{-5}
	c	2.89×10^{-5}
	volume	5.16×10^{-5}
20−600	*a*	-4.51×10^{-6}
	b	-2.32×10^{-6}
	c	-2.10×10^{-6}
	volume	-8.92×10^{-6}
600−800	*a*	-8.61×10^{-6}
	b	-6.79×10^{-6}
	c	-6.52×10^{-6}
	volume	-2.19×10^{-5}
20−600 (heating)	average linear expansion	-3.72×10^{-6}
600−90 (cooling)	average linear expansion	-3.66×10^{-6}

The variable temperature XRD data were collected from −150 to 800 °C, and three NPD data were recorded at −100, 20, and 400 °C, respectively. Figure 3 shows the lattice parameters of orthorhombic $TaVO_5$ with temperature, where cell edge *a* decreased over the entire studied temperature range, while *b* and *c* sharply rose up to 14 °C and then decreased above this temperature. It was worth noting that all parameters reduced rapidly above 600 °C, possibly due to the phase transformation detected by DSC and dilatometry determinations. Furthermore this phase transformation was also clearly observed in another of our $TaVO_5$ samples, which was synthesized by a coprecipitation route with 1:1 molar ratio of Ta and V. We calculated the volumetric TECs as 5.16×10^{-5} °C^{-1} below the first phase transition temperature, -8.92×10^{-6} °C^{-1} in the range of 20−600 °C, and -2.19×10^{-5} °C^{-1} above 600 °C (see Table 1). These data are reliable because the relations $\alpha_V = \alpha_a + \alpha_b + \alpha_c$

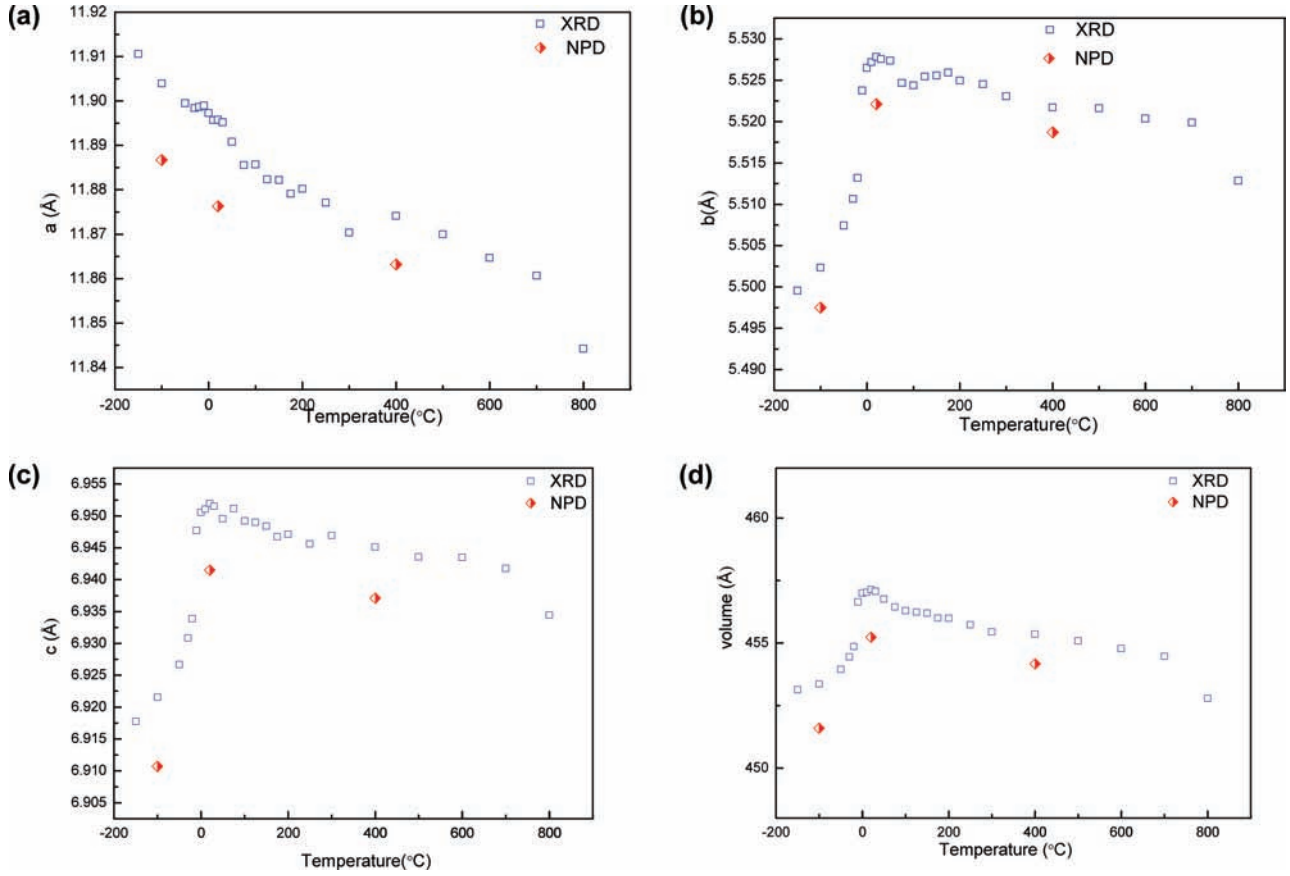

Figure 3. (a) Cell edge *a* variation with temperature. (b) Cell edge *b* variation with temperature. (c) Cell edge *c* variation with temperature. (d) Cell volume variation with temperature from −150 to 800 °C.

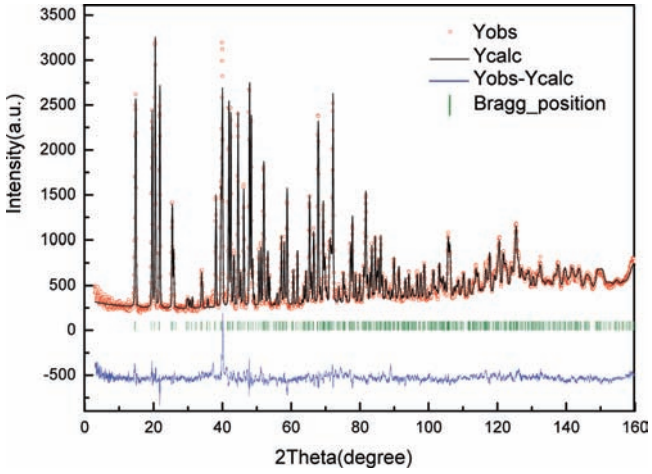

Figure 4. NPD structure refinements of $TaVO_5$ at 20 °C (R_{wp} = 7.26).

and $\alpha_V \approx 3\alpha_1$ are satisfied, where α_1 is linear TEC calculated on dilatometry data.

Preliminary Rietveld refinement with XRD data at 20 °C was carried out on the Fullprof software, fitting 30 parameters such as background coefficients, atomic positions, profile coefficients, anisotropic thermal parameters, etc. The refined result is reasonable because of an acceptable reliable agreement factor (see Figure S2, R_{wp} = 13.7). Thus, the refined Vanadium atomic positions were fixed in the further structure refinements with NPD 3295 data in the 2-θ range of 3−160°, for the almost zero neutron scattering length of Vandium. We obtained the improved structure refinements as shown in Figure 4 and Figure S3, and the refined atomic positions, anisotropic thermal parameters, bond lengths, bond angles, and atomic bond valences at 20 and 400 °C are tabulated in Tables 2−4 and Tables S1−S2.

Table 2. Atomic Positions of $TaVO_5$ at 20 and 400 °C (In Bold)[a]

atom	site	*x*	*y*	*z*
Ta	4c	0.05883 (10)	0.25000(0)	0.34395 (20)
		0.05894(15)	**0.25000(0)**	**0.34281(29)**
V	4c	0.34845 (20)	0.25000(0)	0.52363 (37)
		0.34845 (20)	**0.25000(0)**	**0.52363 (37)**
O1	4b	0.00000(0)	0.00000(0)	0.50000(0)
		0.00000(0)	**0.00000(0)**	**0.50000(0)**
O2	8d	0.12376 (9)	−0.00266 (25)	0.15791 (20)
		0.12344(15)	**-0.00281(35)**	**0.15752(28)**
O3	4c	0.20407 (11)	0.25000(0)	0.47239 (24)
		0.20423(16)	**0.25000(0)**	**0.47172(36)**
O4	4c	0.42315 (13)	0.25000(0)	0.32116 (25)
		0.42183(19)	**0.25000(0)**	**0.32174(39)**

[a] The atomic positions of V atom and the corresponding standard deviations were from the XRD refinement result at 20 °C.

The framework of orthorhombic $TaVO_5$ is composed of TaO_6 and VO_4 polyhedra. Each TaO_6 octahedron is connected with

Table 3. Bond length in $TaVO_5$ at 20 and 400 °C (In Bold)

Ta−O1 × 2	Ta−O2 × 2	Ta−O3 × 1	Ta−O4 × 1
1.8887	2.0516	1.9417	1.9774
1.8925↑	**2.0455↓**	**1.9418**	**1.9871↑**
V−O2 × 2	V−O3 × 1	V−O4 × 1	
1.6862	1.7512	1.6620	
1.6837↓	**1.7484↓**	**1.6490↓**	
V-(O2)- Ta	V-(O3)- Ta	V-(O4)- Ta	
3.7121	3.6588	3.5711	
3.7045↓	**3.6564↓**	**3.5633↓**	
Ta-(O1)- Ta	Ta - Ta	V- V	
3.7775	5.6901	4.5485	
3.7849↑	**5.6736↓**	**4.5443↓**	

Table 4. Bond angles of $TaVO_5$ at 20 and 400 °C (In Bold)

O1−Ta−O1	O1−Ta−O2	O1−Ta−O3	O1−Ta−O4	O1−Ta−O2
93.928	90.170	93.743	91.774	175.654
93.611↓	**90.173**	**93.589↓**	**91.637↓**	**175.968↑**
O2−Ta−O2	O2−Ta−O3	O2−Ta−O4	O3−Ta−O4	
85.699	87.428	86.644	171.911	
86.011↑	**87.555↑**	**86.860↑**	**172.361↑**	
O2−V−O2	O2−V−O3	O2−V−O4	O3−V−O4	
108.195	107.693	111.282	110.543	
108.236↑	**107.904↑**	**111.343↑**	**109.978↓**	
V−O2−Ta	V−O3−Ta	V−O4−Ta	Ta−O1−Ta	
166.506	164.385	157.684	180.000	
166.744↑	**164.464↑**	**156.924↓**	**180.000**	

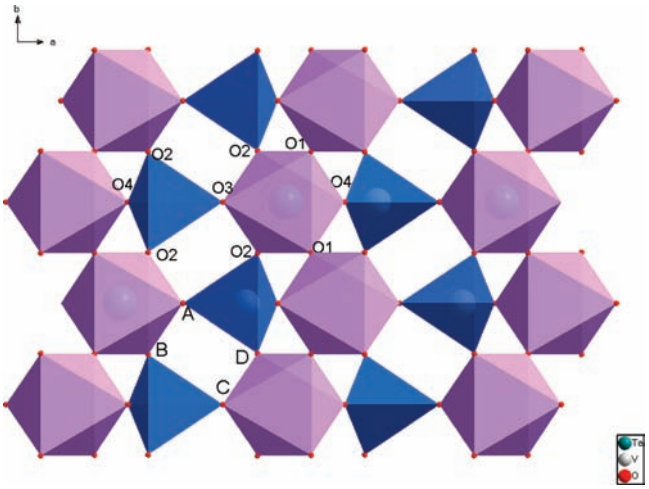

Figure 5. Structure of $TaVO_5$ in ⟨001⟩.

two other TaO_6 octahedra and four VO_4 tetrahedra by sharing the corner oxygen, and each VO_4 is linked by four TaO_6 octahedra. The 180° angle of Ta−O1−Ta indicates the TaO_6 octahedron array in a zigzag along the *b* axis (see Figure 5). Above 20 °C, negative thermal expansions were observed in all three-cell dimensions. However, the angle of the linkage of Ta−O−V increases with temperature rising (see Table 3), which

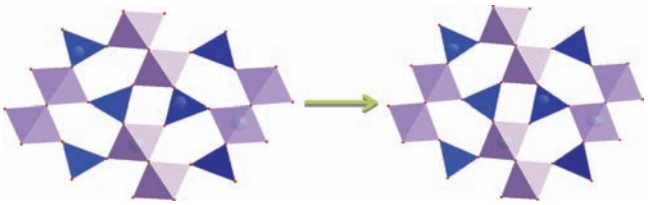

Figure 6. NTE demonstration with temperature increasing of $TaVO_5$ in ⟨0 1 0⟩.

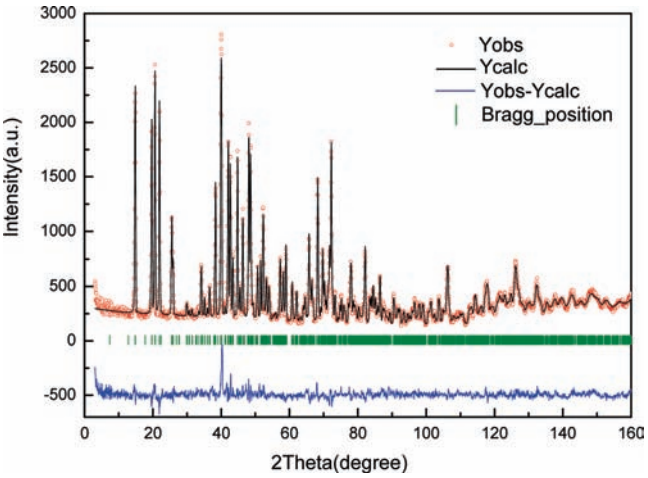

Figure 7. NPD structure refinements of $TaVO_5$ at −100 °C (R_{wp} = 7.06).

Table 5. Atomic Positions of $TaVO_5$ at −100 °C[a]

atom	*x*	*y*	*z*
Ta1	0.43996 (42)	0.25481 (125)	0.29650 (39)
Ta2	0.94163 (31)	0.25306 (88)	0.14292 (32)
V1	0.14956 (59)	0.21601 (293)	0.05124 (66)
V2	0.65688 (58)	0.26470 (473)	0.09231 (65)
O1	−0.00511 (48)	−0.03039 (125)	0.23400 (42)
O2	0.50804 (53)	0.46981 (88)	0.24778 (49)
O3	0.87725 (51)	0.03338 (146)	0.00396 (47)
O4	0.88065 (54)	0.53648 (120)	0.03507 (47)
O5	0.38239 (49)	0.53661 (151)	0.35274 (56)
O6	0.36903 (36)	0.02672 (95)	0.36543 (43)
O7	0.79426 (38)	0.24454 (93)	0.13297 (38)
O8	0.29655 (46)	0.26090 (182)	0.15926 (50)
O9	0.57454 (40)	0.25381 (132)	0.44707 (42)
O10	0.07860 (41)	0.28546 (116)	0.12604 (54)

[a] The atomic positions of V atom and the corresponding standard deviations were from the XRD refinement result.

means that the transverse thermal vibration model cannot be explained for the NTE mechnism here. It is noticed that bond lengths of V−O2, V−O3, and V−O4 decrease with temperature. The shrinkage of VO_4 tetrahedron gives rise to the angles changes of V−O−Ta with temperature. The tilting of TaO_6 and VO_4 polyhedra might result in negative thermal expansion (see Figure 6).

The phase transformation at −14 °C was determined by XRD and NPD data refinements. After many tests and trying fitting with various possible space groups according to transformation

Table 6. Anisotropic Thermal Parameters (Å^2) of $TaVO_5$ at −100 °C

atom	10000*U11	10000*U22	10000*U33
Ta1	46(3)	134(12)	14(2)
Ta2	4(2)	4(0)	1(0)
V1	0	0	0
V2	0	0	0
O1	18(2)	247(21)	4(0)
O2	35(3)	3(0)	37(3)
O3	33(3)	429(31)	3(0)
O4	69(4)	149(21)	2(0)
O5	27(3)	225(24)	43(4)
O6	2(0)	74(15)	32(3)
O7	12(2)	2(0)	7(2)
O8	8(2)	480(24)	24(4)
O9	27 (3)	193(21)	5(3)
O10	10(3)	170(23)	34(4)

matrix and the isostructural with $NbPO_5$,[7] the reasonable structure of the low temperature phase is chose as a monoclinic structure with space group $P2_1/c$. Figure 7 shows the NPD data refined results with a reliable agreement factor (R_{wp} = 7.06) at −100 °C. The calculated cell constants are a = 13.7349, b = 5.4964, c = 13.8196, and β = 120.083°. The low temperature phase (−100 °C) structure parameters, involving atomic positions, anisotropic thermal parameters, bond lengths, bond angles, and atomic bond valences, are listed in Tables 5−8 and Table S3. Similarly, vanadium atomic positions are retrieved from the XRD data refinement at −100 °C (see Figure S4). As shown in Figure 8, the rigid 180° angles of Ta−O−Ta in orthorhombic bend to be Ta2−O1−Ta2 (163.733°) and Ta1−O2−Ta1 (166.359°) in monoclinic. Also the equal bond length of Ta−O in high temperature phase changes into different lengths such as Ta1−O2, Ta2−O1, etc. The rigid TaO_6 octahedron in orthorhombic becomes nonregular and soft octahedral in monoclinic. The softened octahedra results in the tilting and coupling between TaO_6 and VO_4 polyhedra, leading to the structure

Table 7. Bond Lengths of $TaVO_5$ at −100 °C

Ta1−O2 × 1	**Ta1−O2 × 1**	**Ta1−O5 × 1**	**Ta1−O6 × 1**	**Ta1−O8 × 1**	**Ta1−O9 × 1**
1.8308	1.9435	2.0601	2.0881	1.9317	1.9723
Ta2−O1 × 1	**Ta2−O1 × 1**	**Ta2−O3 × 1**	**Ta2−O4 × 1**	**Ta2−O7 × 1**	**Ta2−O10 × 1**
1.8930	1.9040	2.0551	2.0240	1.9587	2.0168
V1−O3 × 1	**V1−O4 × 1**	**V1−O8 × 1**	**V1−O10 × 1**		
1.5215	1.7173	1.8290	1.7821		
V2−O5 × 1	**V2−O6 × 1**	**V2−O7 × 1**	**V2−O9 × 1**		
1.6889	1.6585	1.6811	1.7438		

Table 8. Bond Angles of $TaVO_5$ at −100 °C

O2−Ta1−O2	**O2−Ta1−O5**	**O2−Ta1−O6**	**O2−Ta1−O8**	**O2−Ta1−O9**
93.940	90.938	174.912	94.876	90.523
O2−Ta1−O5	**O2−Ta1−O6**	**O2−Ta1−O9**	**O5−Ta1−O6**	**O8−Ta1−O2**
174.849	89.373	91.859	85.649	93.422
O8−Ta1−O5	**O8−Ta1−O6**	**O8−Ta1−O9**	**O9−Ta1−O5**	**O9−Ta1−O6**
87.805	88.771	172.168	86.436	85.506
O1−Ta2−O1	**O1−Ta2−O3**	**O1−Ta2−O3**	**O1−Ta2−O4**	**O1−Ta2−O4**
93.956	175.951	88.826	90.684	175.331
O1−Ta2−O7	**O1−Ta2−O7**	**O1−Ta2−O10**	**O1−Ta2−O10**	**O4−Ta2−O3**
94.153	93.886	90.701	94.417	86.513
O7−Ta2−O3	**O7−Ta2−O4**	**O7−Ta2−O10**	**O10−Ta2−O3**	**O10−Ta2−O4**
88.587	86.283	170.069	86.146	84.999
O3−V1−O4	**O3−V1−O8**	**O3−V1−O10**	**O4−V1−O8**	**O4−V1−O10**
116.877	114.979	114.707	104.112	102.774
O10−V1−O8	**O5−V2−O9**	**O6−V2−O5**	**O6−V2−O7**	**O6−V2−O9**
101.436	107.764	108.213	110.034	109.030
O7−V2−O5	**O7−V2−O9**	**Ta2−O1−Ta2**	**Ta1−O2−Ta1**	**V1−O3−Ta2**
111.029	110.694	163.733	166.359	151.687
V1−O4−Ta2	**V2−O5−Ta1**	**V2−O6−Ta1**	**V2−O7−Ta2**	**V1−O8−Ta1**
170.972	176.006	156.032	165.644	164.648
V2−O9−Ta1	**V1−O10−Ta2**			
159.846	149.519			

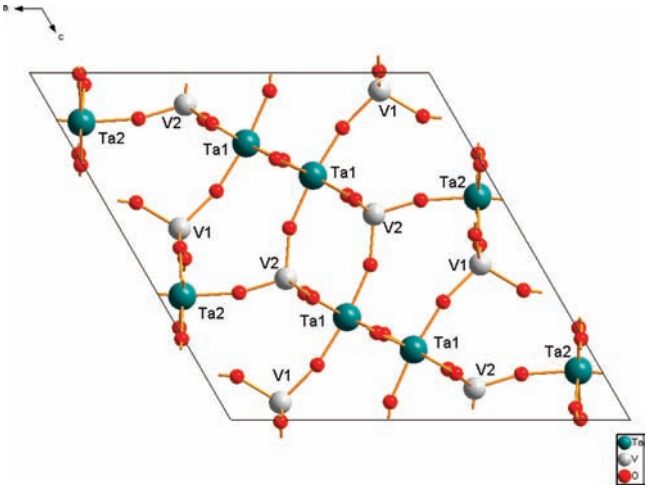

Figure 8. Structure of $TaVO_5$ at −100 °C in ⟨0 1 0⟩.

symmetry decreased during the phase transformation. One can observe that the atoms in the monoclinic cell are two times in the orthorhombic cell, because the monoclinic cell could be divided into two orthorhombic subcells (see Figure 8).

The phase transformation detected by DSC and dilatometric measurements above 600 °C is presumed to be a displacive transition from orthorhombic to tetragonal. The increased anisotropic thermal parameters (Table S2) with temperature indicate the raised structure symmetry possibly. The tetragonal phases with the higher symmetry structure were observed in the isomorphous compound $NbPO_5$, which had two different structures, orthorhombic type, and tetragonal type, though they were synthesized by different thermal treatments.[7,11] The detailed structure and transition mechanism will be studied in the future by further NPD data refinements at high temperature.

CONCLUSIONS

$TaVO_5$ is a negative thermal expansion material above room temperature. The calculated volumetric TECs are -8.92×10^{-6} °C^{-1} in the temperature range of 20−600 °C, and -2.19×10^{-5} °C^{-1} above 600 °C. The NTE behavior is accounted for by the tilting of the TaO_6 and VO_4 polyhedra, which the shrinkage of the VO_4 gives rise to the changes of V−O−Ta angles on heating, while the angle of Ta−O1−Ta maintains at 180° in the framework structure. The phase transformation at −14 °C was revealed by XRD, NPD, and DSC measurements. Below this temperature $TaVO_5$ is a monoclinic structure with space group $P2_1/c$, where rigid TaO_6 octahedron in orthorhombic phase becomes nonregular and soft, and results in the transition from *Pnma* to $P2_1/c$. However, the phase transformation detected around 600 °C has not been identified and the further detailed evidence will be determined in the future.

ASSOCIATED CONTENT

Supporting Information. Atomic bond valences of $TaVO_5$ at −100 °C, 20 and 400 °C; anisotropic thermal parameters (Å^2) of $TaVO_5$ at 20 and 400 °C; dilatometric measurements of $TaVO_5$ in the temperature rang of RT−800 °C; Rietveld refinement with XRD data at 20 °C and −100 °C; Rietveld refinement with NPD data at 400 °C. This material is available free of charge via the Internet at http://pubs.acs.org.

AUTHOR INFORMATION

Corresponding Author
*E-mail: xing@ustb.edu.cn.

ACKNOWLEDGMENT

This work was financially supported by the National Natural Science Foundation of China (20731001, 50725415, 50904003 and 50974015).

REFERENCES

(1) Chahboun, H.; Groult, D. *J. Solid State Chem.* **1986**, *65*, 331–342.
(2) Brown, J. J.; Hummel, F. A. *Trans. Brit. Ceram. Soc.* **1965**, *64*, 419–437.
(3) Labbe, P.; Goreaud, M.; Raveau, B. *J. Solid State Chem.* **1986**, *61*, 324–331.
(4) Amarilla, J. M.; Perez-Revenga, M. L.; Casal, B.; Ruiz-Hitzky, E. *Catal. Today* **2003**, *78*, 571–579.
(5) Amarilla, J.-M.; Casal, B. *Chem. Mater.* **1992**, *4*, 62–67.
(6) Gamba, A., Colella, C. Coluccia, S., Eds. *Studies in Surface Science and Catalysis 155*; Elservier B.V, 2005; pp 427−439.
(7) Amos, T. G.; Sleight, A. W. *J. Solid State Chem.* **2001**, *160*, 230–238.
(8) Chahboun, H.; Groult, D.; Raveau, B. *Mater. Res. Bull.* **1988**, *23*, 805–812.
(9) Chu, C. N.; Saka, N.; Suh, N. P. *Mater. Sci. Eng.* **1987**, *95*, 303–308.
(10) Chu, C. N.; Saka, N.; Suh, N. P. *J. Eng. Mater. Technol.* **1986**, *108*, 275–277.
(11) Amos,T. G. Ph.D Dissertation, Oregon State University, 2001.
(12) Rodriguez-Carjaval, J. Abstracts of the Satellite Meeting on Powder Diffraction of the XVth Congress International Union of Crystallography Toulouse, France, 1990; 127.
(13) Schadow, H.; Oppermann, H.; Wehner, B. *Cryst. Res. Technol.* **1992**, *5*, 691–695.